

# MOBILITY NETWORKED TIME-SERIES FORECASTING BENCHMARK DATASETS

**Anonymous authors**

Paper under double-blind review

## ABSTRACT

Human mobility is crucial for urban planning (e.g., public transportation) and epidemic response strategies. However, existing research often neglects integrating comprehensive perspectives on spatial dynamics, temporal trends, and other contextual views due to the limitations of existing mobility datasets. To bridge this gap, we introduce **MOBINS (MOBility Networked time Series)**, a novel dataset collection designed for networked time-series forecasting of dynamic human movements. **MOBINS** features diverse and explainable datasets that capture various mobility patterns across different transportation modes in four cities and two countries and cover both transportation and epidemic domains at the administrative area level. Our experiments with nine baseline methods reveal the significant impact of different model backbones on the proposed six datasets.

## 1 INTRODUCTION

Diverse and explainable human mobility datasets are crucial for advancing urban planning, affecting public transportation demand (Han et al., 2022), crowd congestion (Singh et al., 2020), traffic management (Liu et al., 2024), and infection prediction (Panagopoulos et al., 2021). Previous research focused on forecasting traffic and crowd congestion in specific areas using various transportation modes, such as subway systems (TianChi, 2019), ride-hailing services (Fivethirtyeight, 2015), and taxis (TLC, 2009). Additionally, there have been several attempts to predict COVID-19 infection by analyzing human mobility across different regions (Katragadda et al., 2022).

However, the datasets used in prior studies often fail to capture the diverse nature of human mobility from multiple perspectives. To comprehensively represent diverse mobility patterns, it is imperative to observe the movements of a large number of individuals over an extended period, taking into account various transportation modes. Unfortunately, many studies attempt to estimate demand using data either in a single transportation mode or in a short time frame (TianChi, 2019; Panagopoulos et al., 2021). Some efforts to understand human mobility rely on sparse movement data collected from a limited number of individuals. Despite the importance of understanding human mobility’s impact on various aspects, such as transportation and epidemics, there is a lack of research that integrates additional information beyond transportation to enhance the diversity of mobility datasets.

Subway datasets (TianChi, 2019), a networked mobility dataset consisting of stations with high human traffic volumes, meet many of the specified criteria. Nevertheless, the subway datasets themselves do not offer multiple perspectives—i.e., diversity. Although there have been several studies to broaden a single data perspective (Shi et al., 2020), they only integrate mobility data from a *single* source with other contextual information that shares the same static topology. It is insufficient, for example, to simply add weather information as an additional variable to the time series. Instead, it is critical to use mobility-effected information at specific points of interest (PoIs) to *create synergy* between dynamic movements and networked time series. This approach not only enhances performance but also aids in understanding social phenomena that are difficult to discern from a single data source.

To improve the diversity of human mobility datasets, it is essential to collect data from different transportation modes across diverse regions over an extended period, capturing numerous daily movements. Moreover, incorporating additional contextual information, such as disease outbreaks, can aid in capturing various contextual patterns associated with spatio-temporal information. Meanwhile, for explainability purposes, the instances in the dataset should be organized on a network based on the spatial connectivity of each explainable area unit, such as an administrative area.

054  
055  
056  
057  
058  
059  
060  
061  
062  
063  
064  
065  
066  
067  
068  
069  
070  
071  
072  
073  
074  
075  
076  
077  
078  
079  
080  
081  
082  
083  
084  
085  
086  
087  
088  
089  
090  
091  
092  
093  
094  
095  
096  
097  
098  
099  
100  
101  
102  
103  
104  
105  
106  
107

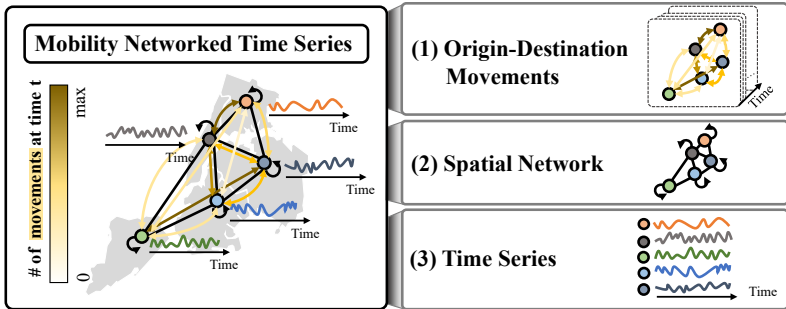


Figure 1: A structure of mobility networked time series in New York. **MOBINS** contains three components: (1) human movements from an origin to a destination over time, (2) spatial structure based on geographic proximity or a road network, and (3) time-varying features (e.g., numbers of taxi pick-ups and drop-offs) of each region. The first and third components cover the same period.

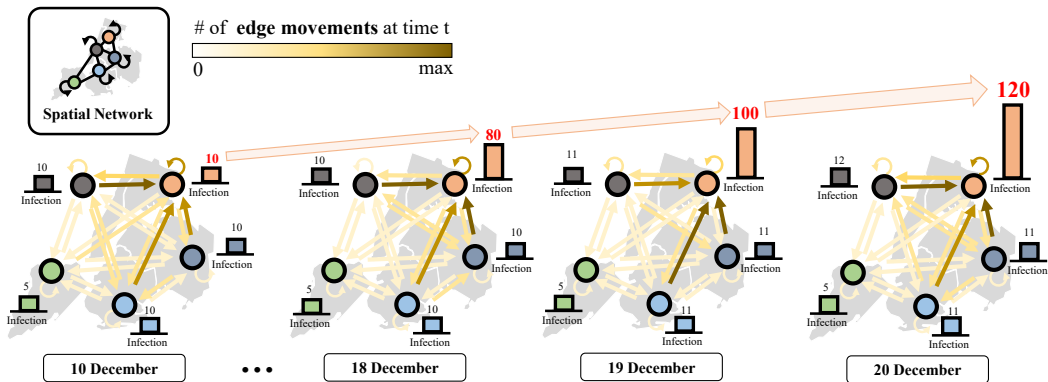


Figure 2: Dynamic edge movements and time-varying infection cases on a static spatial network. On top of the spatial network, node features represent the number of confirmed cases in each city or district over time, and edge features represent population movement flows between cities or districts over time. The increasing number of infection cases at the upper-right node is influenced by the increasing population flows to that node from other nodes.

Towards diverse and explainable human mobility datasets, we propose **MOBINS**, **MOBility Networked time-Series forecasting benchmark**. **MOBINS** offers a unique combination of origin-destination movements, a spatial network, and multiple time series, as illustrated in Figure 1. It involves multiple transportation modes including buses, subways, express buses, and taxis, providing a rich representation of human mobility patterns. With observations spanning at least two years and numerous daily movements, **MOBINS** enables the development and evaluation of advanced forecasting models. To ensure broad applicability, we include the benchmark datasets for transportation and infection prediction across four cities and two countries. By representing the networked mobility datasets at the administrative area level and treating each node as a distinct entity, **MOBINS** helps the model interpretation of the underlying mobility patterns.

Our dataset collection contains not only network-based interactions between nodes and edges but also temporal dynamics from time-varying features. Also, all datasets have a spatial network, where nodes represent locations such as stations, districts, and cities and edges represent connectivity between nodes based on subway lines, roads, and geographical adjacency. In Figure 2 visualizing part of a dataset in **MOBINS**, a spatial network created based on road network information is given as static data, and dynamic human mobility is represented through dynamic edge movements. In this case, the positive correlation between human movements and time-varying infection cases is captured. This kind of insight is difficult to uncover from a straightforward collection of multiple datasets, because their regions, spatial and temporal resolutions, and collection intervals may not be aligned. Therefore, this *new opportunity* clearly demonstrates the innovation and significance of **MOBINS**.

Our sophisticated and diverse dataset collection is publicly available together with forecasting methods. A substantial amount of time and effort has been dedicated to gathering comprehensive

108 datasets from various data sources, as well as merging and preprocessing them in preparation for their  
 109 release. We aspire to contribute to the progress of the community that studies human mobility. Our  
 110 contributions are as follows:

- 111
- 112 • **Datasets:** To the best of our knowledge, this is the first comprehensive dataset collection charac-  
 113 terized by diversity and explainability for mobility networked time-series forecasting.
- 114 • **Experiments:** We conduct experiments to predict both time series and origin-destination move-  
 115 ments. These experiments are based on various baselines with different backbones, applied to our  
 116 dataset collection: transportation and epidemic datasets in four cities and two countries.
- 117 • **Takeaways:** Our experiments highlight the need for an integrated framework that simultaneously  
 118 considers the three components—origin-destination movements, a spatial network, and multiple  
 119 time series—in Figure 1. These insights guide future research directions in developing advanced  
 120 frameworks for mobility networked time-series forecasting.

## 121 2 PRELIMINARIES

### 122 2.1 FORECASTING WITH TRANSPORTATION TIME-SERIES DATA

123  
 124 Human mobility prediction aims to predict each location’s various attributes such as speed, demand,  
 125 and congestion. In the context of traffic forecasting, studies employ traffic speed sensor datasets (Liu  
 126 et al., 2024; Li et al., 2017) collected from PeMS (Performance Measurement System). Similarly,  
 127 studies on demand or congestion prediction use modified inflow and outflow datasets derived from  
 128 various transportation modes, such as subway (TianChi, 2019) or taxi (TLC, 2009) datasets. Unlike  
 129 conventional time-series forecasting, mobility time-series forecasting emphasizes both temporal and  
 130 spatial modules. Spatial axes are represented using  $N \times N$  grids based on given coordinates, while  
 131 an adjacency graph captures spatial connectivity derived from PoIs or a correlation generated from  
 132 the sensor proximity (Jiang et al., 2021). Alternatively, station-based spatial connectivity is employed  
 133 to model the patterns of movements within a given graph (Ou et al., 2020).  
 134  
 135

### 136 2.2 FORECASTING WITH ORIGIN-DESTINATION DATA

137  
 138 Origin-destination (OD) forecasting focuses on predicting the number of movements between the  
 139 regions, capturing the interaction patterns within a mobility network. Datasets from ride-hailing  
 140 services (Fivethirtyeight, 2015), taxi (TLC, 2009), and subway (TianChi, 2019) provide valuable  
 141 information for deriving origins and destinations. OD movements between candidate origins and  
 142 destinations, such as grids, stations, and PoIs, are forecasted using spatial and temporal modules (Han  
 143 et al., 2022; Wang et al., 2019; Rong et al., 2023). Meanwhile, several studies have attempted to  
 144 enhance time-series forecasting performance by incorporating OD movements. For example, research  
 145 on COVID-19 prediction in England (Panagopoulos et al., 2021) and USA (Wang et al., 2023) has  
 146 used the interaction between nodes, represented by the number of COVID-19 cases, and human  
 147 mobility between regions. These studies leverage the relationship between inter-regional movement  
 148 and the spread of infections to predict the number of cases in each region (Katragadda et al., 2022).  
 149

## 150 3 MOBILITY NETWORKED TIME SERIES

### 151 3.1 PROBLEM DEFINITIONS

152  
 153 Mobility is represented along both spatial and temporal dimensions. The spatial component is  
 154 structured through a graph, denoted as  $G = (V, E)$ . The node set  $V = \{v_1, v_2, \dots, v_N\}$  captures  
 155 locational data, while the edge set  $E$  illustrates the connectivity between these nodes. Each node  
 156 temporally aggregates *node time-series features*  $X_t$ , encompassing metrics such as transportation  
 157 in/out-flow, ridership, infection rates, and additional time-sensitive data, where  $X_t \in \mathbb{R}^{N \times d}$ ,  $d$  is the  
 158 number of feature variables, and  $t$  is the index of the time. In scenarios where the graph  $G$  remains  
 159 static, its *spatial network*  $A \in \mathbb{R}^{N \times N}$  is defined through a fixed adjacency matrix. Conversely, in  
 160 dynamic settings,  $G$  evolves with *OD movements*  $M_t \in \mathbb{R}^{N \times N}$ , where  $M_t^{ij}$  accurately measures the  
 161 volume of movements from node  $v_i$  to node  $v_j$  at each time point  $t$ .

Table 1: Comparisons based on the components of mobility networked time series (M: million).

Datasets	Spatial Nodes	Spatial Network		OD Movements		Node Time-Series Features		Time Period	
		Edges	Domain	Daily Movements	Modes	Daily Amounts	Domain		
Hangzhou Subway (TianChi, 2019)	81	85	Station	2.9M	Subway	2.9M	Subway In/Out-flow	01/01/2019 – 01/25/2019	
LargeST (CA) (Liu et al., 2024)	8600	201363	Distance	-	-	187.77M	Traffic Flow	01/01/2017 – 12/31/2021	
COVID (England) (Panagopoulos et al., 2021)	129	-	-	11.86M	Mobile Device	1975	Infection	03/01/2020 – 04/30/2020	
MOBINS (Transportation)	Seoul	128	290	Station-based Administrative Area	2.68M	Smart Cards	4.02M	Subway In/Out-flow	01/01/2022 – 12/31/2023
	Busan	60	121		0.63M		0.75M		
	Daegu	61	123		0.25M		0.34M		
	NYC	5	12	Borough	0.10 M	Taxi	3.03M	Ridership	02/01/2022 – 03/31/2024
MOBINS (Epidemic)	Korea	16	45	City & Province	13.41M	Smart Cards	25834	Infection	01/20/2020 – 08/31/2023
	NYC	5	12	Borough	2418	Taxi	2038	Infection	03/01/2020 – 12/31/2023

Table 2: Comparisons based on crucial criteria for mobility datasets.

Datasets	Diversity (§3.2.1)					Explainability (§3.2.2)	
	Various Modes	Various Regions	Long Period	Many Daily Movements	Bi-Modal Dataset	Explainable Units	Spatial Network
Hangzhou Subway (TianChi, 2019)	X	X	X	O	O	O	O
LargeST (Liu et al., 2024)	O	O	O	-	X	X	O
COVID (Panagopoulos et al., 2021)	O	O	X	O	O	O	X
<b>MOBINS</b>	O	O	O	O	O	O	O

**Definition 3.1** (MOBILITY NETWORKED TIME-SERIES FORECASTING). Given a spatial network  $A$  and a corresponding historical dataset  $D = \{D_1, D_2, \dots, D_T\}$ , where  $D_t = (X_t, M_t)$  includes node time-series features  $X_t$  and OD movements  $M_t$ , the objective of *mobility networked time-series forecasting* is to learn a function  $f$  that forecasts both the future node times-series features  $\{X_{T+1}, X_{T+2}, \dots, X_{T+H}\}$  and the future OD movements  $\{M_{T+1}, M_{T+2}, \dots, M_{T+H}\}$  over a forecast horizon  $H$ .

### 3.2 LIMITATIONS OF EXISTING MOBILITY DATASETS

Existing mobility datasets, as used in human mobility forecasting, are compared with the characteristics of our **MOBINS** in Table 1. We categorize existing human mobility datasets into three types. In the first type, the Hangzhou Subway dataset (TianChi, 2019) offers deep analysis through individual unit data but is limited by its specific region and short collection period, sharing the limitation also observed in datasets like the NYC Uber dataset (Fivethirtyeight, 2015). This dataset’s collection from a single source makes it challenging to capture the diverse nature of human mobility. In the second type, LargeST (Liu et al., 2024) provides extensive data over a long collection period but lacks detailed human mobility information, such as OD movements. This limitation is also present in other PeMS-based datasets, such as the MERA-LA and PEMS-BAY datasets (Li et al., 2017). In the third type, Panagopoulos et al. (2021) shared human mobility datasets that link movements with other factors. However, its short collection period makes it challenging to observe long-term trends, and the absence of a spatial network reduces its utility for spatial analysis.

For urban planning purposes (e.g., public transportation) and epidemic response strategies, human mobility datasets should provide multiple views of spatial and temporal dimensions, as well as exhibit qualities such as diversity and explainability. However, many of the datasets currently available do not meet these criteria. In Table 2, we highlight the specific shortcomings of existing human mobility datasets, emphasizing their deficiencies in capturing essential qualities.

216  
217  
218  
219  
220  
221  
222  
223  
224  
225  
226  
227  
228  
229  
230  
231  
232  
233  
234  
235  
236  
237  
238  
239  
240  
241  
242  
243  
244  
245  
246  
247  
248  
249  
250  
251  
252  
253  
254  
255  
256  
257  
258  
259  
260  
261  
262  
263  
264  
265  
266  
267  
268  
269

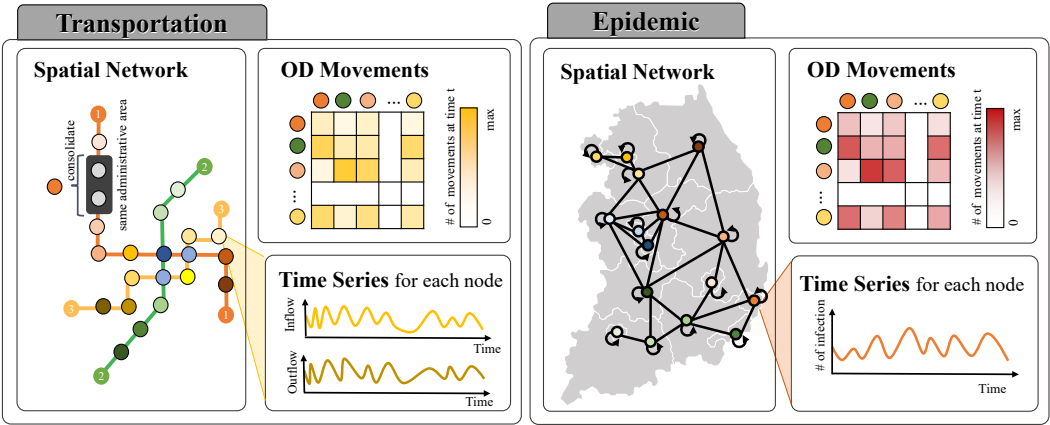


Figure 3: Composition of the transportation and epidemic datasets in South Korea.

### 3.2.1 DIVERSITY

To accurately represent human mobility, datasets should encompass a wide array of contexts. Human movement can occur through various modes of transportation, such as subways, city buses, long-distance buses, high-speed trains, taxis, personal vehicles, and ride-hailing services. A dataset that covers only a single mode of transportation, like the subway dataset (TianChi, 2019), fails to provide a comprehensive view of mobility. Datasets incorporating *various modes* are essential for depicting the diverse nature of human mobility. From a spatial perspective, the mobility datasets should encompass *various regions* to capture the different spatial and contextual patterns, such as commercial, residential, tourist, and mixed-use area patterns, emerging from diverse administrative areas. For instance, COVID datasets (Panagopoulos et al., 2021) cover four EU countries, and LargeST (Liu et al., 2024) includes datasets from across California, including Los Angeles, the Bay Area, and San Diego. From a temporal perspective, datasets should also include *long periods* to offer insights into both short-term and long-term mobility patterns. It is critical that datasets extend beyond simple metrics such as ‘time of day’ or ‘day of the week’ to include annual data, facilitating a richer temporal context. However, except for LargeST (Liu et al., 2024), many datasets cover periods of less than one year, with some training models over periods even shorter than one month (TianChi, 2019; Li et al., 2017). Moreover, mobility datasets must be collected with *many daily movements*. Unfortunately, several datasets are employed with only an insufficient number of daily movements (Wang et al., 2023), which fail to capture representative human mobility. Understanding human movements is not only about comprehending the movements themselves but also about linking information strongly correlated with these movements to get insights into social phenomena, which allows for the exploration of many aspects of human mobility. Therefore, *bi-modality* is helpful to comprehend human movements and their strongly correlated phenomena. For example, the COVID datasets consist of two types of data: OD movements from human mobility between regions based on mobile device data, and node time-series features from the number of infected individuals.

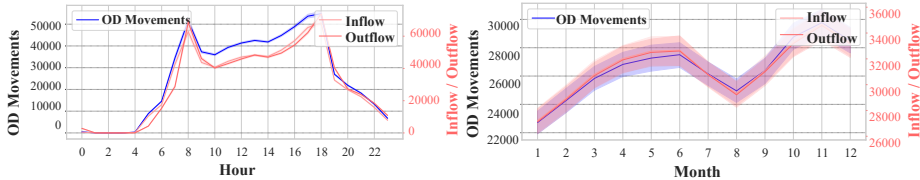
### 3.2.2 EXPLAINABILITY

Decision-makers in urban planning require models with high explainability, which necessitates datasets with inherent explainability. Training models using grid or sensor identifiers (Li et al., 2017; Liu et al., 2024) is insufficient. *Explainable units* for locational information, e.g., administrative areas, are vital. In the spatial dimension of mobility, each dataset should realistically represent spatial connectivity. For instance, the subway dataset (TianChi, 2019) records connectivity at the station level. Administrative areas can create a *spatial network* based on actual spatial adjacency and connectivity, indirectly helping to understand how the impact of an event spreads out.

## 4 DATASET COLLECTION: MOBINS

Our **MOBINS** dataset collection encompasses two domains: *transportation* and *epidemic*.

270  
271  
272  
273  
274  
275  
276  
277  
278  
279  
280  
281  
282  
283  
284  
285  
286  
287  
288  
289  
290  
291  
292  
293  
294  
295  
296  
297  
298  
299  
300  
301  
302  
303  
304  
305  
306  
307  
308  
309  
310  
311  
312  
313  
314  
315  
316  
317  
318  
319  
320  
321  
322  
323



(a) [Hours of the day] Average and 95% C.I. (b) [Months of the year] Average and 95% C.I.

Figure 4: Temporal patterns with positive correlations between inflow/outflow and OD movements about different periods in *Transportation-Busan*. Inflow/outflow and OD movements on all nodes are aggregated hourly or monthly to calculate the average and 95% confidence interval (C.I.).

#### 4.1 DATASET CONSTRUCTION

**Transportation datasets:** The **MOBINS** dataset collection comprises transportation data from three South Korea cities (Seoul, Busan, and Daegu) and one U.S. city (New York City). The *Transportation-[Seoul, Busan, Daegu]* datasets include node time-series features from subway inflow/outflow data and OD movements from smart card usage across various public transportation modes. These datasets use subway maps to represent spatial connectivity, leveraging the commonalities between node time-series features and OD movements. However, pre-processing is required to align the data to a consistent spatial and hourly resolution, as node time-series features are generated for each station and OD movements are based on administrative areas. Figure 3 illustrates that stations within the same administrative area are consolidated into a single node in the spatial network, resulting in nodes represented by station-based administrative areas. The *Transportation-NYC* dataset includes OD movements from the NYC yellow and green taxi datasets (TLC, 2009) and node time-series features from NYC subway, tram, and railway ridership data. The spatial network is built at the borough level to alleviate sparsity from the huge number of nodes. Consequently, NYC taxi records from 263 zones and NYC ridership data from 428 stations are represented at a consistent resolution.

**Epidemic datasets:** The **MOBINS** dataset collection includes epidemic datasets that consist of node time-series features obtained from COVID-19 infection count and OD movements obtained from a smart card or taxi trip records in South Korea or New York City (NYC). The ‘Epidemic’ section in Figure 3 illustrates the composition of the *Epidemic-Korea* dataset based on the spatial networks characterized by an adjacency matrix with diagonal ones representing the connectivity between cities and provinces. The OD movements from buses, urban rails, railways, and long-distance buses are used to represent inter-city or inter-provincial movements. However, islands are excluded due to their distinct transportation modes. Each node represents a city or a province, with COVID-19 infection cases recorded at each administrative area. Similarly, for the *Epidemic-NYC* dataset, node time-series features are based on daily infection cases from the five boroughs, while OD movements are comprehensively integrated from the NYC yellow and green taxi datasets (TLC, 2009).

#### 4.2 DATASET STRAWMAN ANALYSIS

**Transportation datasets:** Figure 4 illustrates both the ‘hours of the day’ and ‘months of the year’ patterns in the *Transportation-Busan* dataset, using the long-term data collection spanning at least two years. The dataset exhibits a strong positive correlation between OD movements and node time-series features, as evident from the similar temporal distributions. Though these two modalities may show different values at a fine granularity, their aggregated trends coincide with each other, which confirms the validity of the dataset. Common temporal patterns include commuting patterns at 8 a.m. and 6 p.m., where both OD movements and inflow/outflow reach their peak values, as shown in Figure 4a. Also, these temporal patterns in Figures 4a and 4b highlight the importance of capturing both short-term and long-term dynamics in mobility networked time-series forecasting. From a spatial perspective, Figure 5a displays the total sum of OD movements between nodes, and Figure 5b is a matrix based on hops, indicating the number of nodes to be traversed from one node

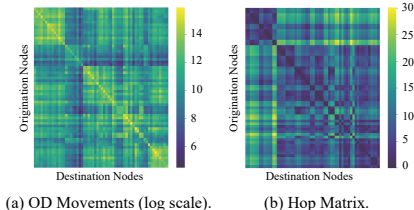


Figure 5: Spatial patterns of the OD movements and hop matrix in the *Transportation-Busan* dataset.

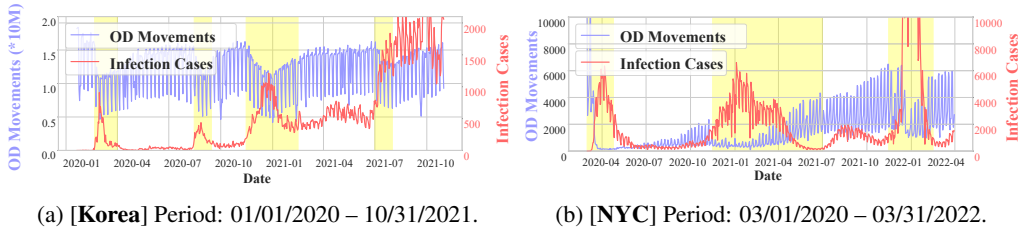


Figure 6: Temporal patterns show negative relationships between infection cases and OD movements in the *Epidemic-[Korea, NYC]* datasets. The negative correlation is prominent in the yellow background. Infection cases and OD movements about all nodes are summed daily (M: million).

Table 3: Dataset statistics and default configurations. ‘# Node’ is the number of nodes which indicate regions (e.g., stations or PoIs). We newly define forecasting target attributes with node time-series features and OD movements. For every node, the ‘Target Dim.’ is defined by  $N^2 + d \cdot N$ , where  $N$  is the number of regions and  $d$  is the number of feature variables from each node.

Domain	Dataset	# Node	Target Dim.	Total Period	Train Days	Test Days	Time Interval
Transportation	Seoul	128	16640	01/01/2022 – 12/31/2023	548	182	1 hour
	Busan	60	3720	01/01/2021 – 12/31/2023	822	273	1 hour
	Daegu	61	3843				
	NYC	5	30	02/01/2022 – 03/31/2024	593	197	1 hour
Epidemic	Korea	16	272	01/30/2020 – 08/31/2023	990	330	1 day
	NYC	5	30	03/01/2020 – 12/31/2023	1051	350	1 day

to another on the spatial network. Figure 5 reveals a negative correlation between OD movements and the hop matrix. In the hop matrix, darker colors represent a lower number of hops in the spatial network. Conversely, areas with higher (brighter) OD movements are associated with lower (darker) hops in the hop matrix. This finding suggests that a spatial network and OD movements are correlated, with higher mobility observed between nodes that have lower hops.

**Epidemic datasets:** Figure 6 presents the daily COVID-19 infection cases and daily OD movements for the *Epidemic-[Korea, NYC]* datasets. Figures 6a and 6b reveal a negative correlation between infection cases and movements during the early stages of the COVID-19 pandemic. As infection cases increase, human movements decrease, indicating a change in mobility patterns in response to the outbreak. From a temporal perspective, the *Epidemic-[Korea, NYC]* datasets demonstrate a strong negative correlation between node time-series features (infection cases) and OD movements, providing comprehensive insights into the interplay between the spread of infection and human mobility. This temporal analysis emphasizes the importance of considering the dynamic relationship between human mobility and disease spread.

## 5 EXPERIMENTS

Table 3 summarizes the statistics of the datasets used in our experiments.

### 5.1 EXPERIMENTAL SETTINGS

To evaluate our dataset collection with a four-day look-back window and various prediction lengths, we use Mean Absolute Error (MAE) as an evaluation metric, as shown in Table 4. We assess model performance across three different prediction lengths: 7, 14, and 30 days, to capture both short-term and long-term forecasting capabilities. Previous studies have employed prediction lengths ranging from 96 to 720 steps for long-term forecasting and 6 to 48 steps for short-term forecasting (Wu et al., 2022). For *Transportation-[Seoul, Busan, Daegu, NYC]* datasets that have a 1-hour time interval, we evaluate long-term forecasts at horizons of 168, 336, and 720 hours (i.e., 7, 14, and 30 days). Since the 1-hour interval results in many time points, these horizons are considered long-term. Meanwhile, for the *Epidemic-[Korea, NYC]* datasets, which have a 1-day time interval, the same prediction

378 periods of 7, 14, and 30 days represent short-term forecasts. Therefore, our dataset collection serves  
 379 as a comprehensive benchmark for both long-term and short-term mobility networked time-series  
 380 forecasting, depending on the datasets’ time interval, with prediction lengths consistently set to 7,  
 381 14, and 30 days. For fair comparisons, all baselines are configured to follow the same experimental  
 382 setup, running for 10 epochs with early stopping.

## 384 5.2 BASELINES

386 In our evaluation with **MOBINS**, we consider a broad range of traditional and modern forecasting  
 387 models as baselines. We choose well-acknowledged prediction models as our benchmark, including  
 388 (i) Linear-based models: DLinear, NLinear (Zeng et al., 2023); (ii) RNN-based model: SegRNN (Lin  
 389 et al., 2023); (iii) Transformer-based models: Informer (Zhou et al., 2021), Reformer (Kitaev et al.,  
 390 2020), PatchTST (Nie et al., 2022); (iv) CNN-based model: TimesNet (Wu et al., 2022); (v) GNN-  
 391 based models: STGCN (Yu et al., 2018), MPNNLSTM (Panagopoulos et al., 2021).

392 Linear models take a linear approach to forecasting, treating time-series data as linear signals.  
 393 DLinear and NLinear are known for their simplicity and efficiency, focusing on capturing linear  
 394 trends and patterns. The RNN-based model, SegRNN, employs a recurrent neural network to capture  
 395 temporal dependencies in the data. RNNs are well-suited for sequential data and are commonly used  
 396 for time-series forecasting. SegRNN uses a segmentation-based technique to enhance the ability  
 397 to capture long-range dependencies. Transformer-based models use self-attention mechanisms to  
 398 capture long-range dependencies in time-series data. Reformer is an efficient variant of Transformer  
 399 models that replaces dot-product attention with locality-sensitive hashing, reducing complexity and  
 400 employing reversible residual layers to store activations only once during training. PatchTST extends  
 401 the Transformer model to time-series data by breaking down the data into smaller patches. This  
 402 approach allows the model to focus on localized patterns while leveraging the power of self-attention  
 403 to understand broader trends. The CNN-based model, TimesNet, uses convolutional layers to capture  
 404 temporal patterns in the data, allowing it to efficiently process time series with high-dimensional  
 405 features. This model can identify localized patterns effectively, making it suitable for various time-  
 406 series forecasting tasks. The GNN-based models use diverse graphs to deal with spatial information or  
 407 integrate other contextual information for time-series forecasting. STGCN uses a static graph derived  
 408 from inter-node proximity, while MPNNLSTM utilizes a dynamic graph based on OD movements.

## 409 5.3 BASELINE EVALUATION RESULTS

411 In this section, we outline the key results from our experiments, detailing how each baseline performs  
 412 across a range of datasets. The outcomes highlight the relative strengths and weaknesses of different  
 413 forecasting models and offer insights into their applicability in diverse contexts.

- 415 • **Linear models:** DLinear and NLinear demonstrated strong performance, achieving the lowest  
 416 error rates on several datasets. DLinear was the best model for the *Transportation-Daegu* dataset  
 417 across all prediction lengths and for the *Transportation-[Seoul, Busan]* datasets for 14-day and  
 418 30-day predictions. This result suggests that linear models can be highly effective in scenarios  
 419 with simpler data patterns or lower degrees of complexity.
- 420 • **RNN-based models:** SegRNN showed competitive performance but did not achieve the best  
 421 scores on any dataset, indicating that RNNs may face challenges with the increased complexity  
 422 and longer-range dependencies typically associated with some time-series forecasting tasks.
- 423 • **Transformer-based models:** Recent approaches such as Informer, Reformer, and PatchTST  
 424 were assessed. PatchTST excelled in the *Transportation-Seoul* dataset for the 7-day prediction  
 425 length, achieving an average error rate of 0.3995 with a standard deviation of 0.0046. This result  
 426 emphasizes the adaptability and versatility of Transformer-based approaches, which are known for  
 427 their ability to handle long-range dependencies effectively.
- 428 • **CNN-based models:** TimesNet achieved the lowest error rates in several datasets, including  
 429 the *Transportation-[Seoul, NYC]* and *Epidemic-[Korea, NYC]* datasets across all prediction  
 430 lengths. These findings suggest that CNN-based models can be highly effective in certain contexts,  
 431 particularly when dealing with spatio-temporal patterns.
- **GNN-based models:** STGCN and MPNNLSTM were evaluated, but they did not outperform other  
 baseline models in any of the datasets. However, their performance was competitive, indicating



Table 4: Prediction comparison between nine baselines in terms of average MAE and standard deviation (in parentheses) with all prediction lengths (7, 14, and 30 days) in all datasets. The best model across each dataset is highlighted in **bold**. Please note the following abbreviations: ‘‘Pred.’’ means ‘‘Prediction’’, ‘‘Trans.’’ refers to ‘‘Transportation’’ and ‘‘Epic.’’ denotes ‘‘Epidemic’’.

Pred. day	Domain	Dataset	Linear-based		RNN-based	Transformer-based			CNN-based	GNN-based		
			DLinear	NLinear	SegRNN	Informer	Reformer	PatchTST	TimesNet	STGCN	MPNNLSTM	
7 days	Trans.	Seoul	0.3858 (±0.0068)	0.4021 (±0.0003)	0.7022 (±0.0363)	0.9204 (±0.0018)	0.5637 (±0.0315)	0.3995 (±0.0046)	<b>0.3822</b> (±0.0062)	0.4053 (±0.0047)	0.6401 (±0.0009)	
		Busan	<b>0.5743</b> (±0.0056)	0.5898 (±0.0006)	0.9986 (±0.0087)	3.4773 (±0.0031)	0.7316 (±0.0075)	0.6411 (±0.0052)	0.6103 (±0.0642)	0.6945 (±0.0032)	0.9556 (±0.0035)	
		Daegu	<b>0.4677</b> (±0.0004)	0.4919 (±0.0003)	0.7876 (±0.0597)	1.3885 (±0.0038)	0.5338 (±0.0014)	0.4916 (±0.0011)	0.4902 (±0.0087)	0.4901 (±0.0032)	0.7337 (±0.0018)	
		NYC	0.4491 (±0.0011)	0.4460 (±0.0005)	0.9226 (±0.0462)	0.9147 (±0.0077)	0.5503 (±0.0036)	0.4687 (±0.0027)	<b>0.3984</b> (±0.0024)	0.4601 (±0.0019)	0.6627 (±0.0015)	
	Epic.	Korea	0.5767 (±0.0031)	0.5828 (±0.0015)	0.5936 (±0.0072)	1.7884 (±0.0013)	0.7137 (±0.0320)	0.6014 (±0.0392)	<b>0.4133</b> (±0.0058)	0.7427 (±0.0199)	0.7827 (±0.0062)	
		NYC	0.4830 (±0.0016)	0.4666 (±0.0022)	0.4896 (±0.0179)	1.0627 (±0.0015)	0.5945 (±0.0165)	0.5026 (±0.0044)	<b>0.3948</b> (±0.0033)	0.5794 (±0.0038)	0.6934 (±0.0062)	
	14 days	Trans.	Seoul	<b>0.3878</b> (±0.0047)	0.4072 (±0.0003)	0.7183 (±0.0071)	0.6453 (±0.0043)	0.6310 (±0.0105)	0.4006 (±0.0028)	0.4015 (±0.0312)	0.4182 (±0.0257)	0.6399 (±0.0013)
			Busan	<b>0.5830</b> (±0.0075)	0.5934 (±0.0003)	0.9913 (±0.0243)	0.9482 (±0.0012)	0.7434 (±0.0045)	0.6324 (±0.0023)	0.6175 (±0.0611)	0.6862 (±0.0044)	0.9528 (±0.0040)
			Daegu	<b>0.4696</b> (±0.0004)	0.4942 (±0.0004)	0.8154 (±0.0039)	0.7284 (±0.0004)	0.5486 (±0.0045)	0.4919 (±0.0007)	0.4826 (±0.0033)	0.4888 (±0.0021)	0.7323 (±0.0009)
			NYC	0.4579 (±0.0023)	0.4501 (±0.0004)	0.9027 (±0.0237)	0.7229 (±0.004)	0.5623 (±0.0071)	0.4680 (±0.0011)	<b>0.3988</b> (±0.0017)	0.4629 (±0.0023)	0.6624 (±0.0008)
Epic.		Korea	0.6258 (±0.0006)	0.6088 (±0.0010)	0.6484 (±0.0210)	1.0182 (±0.0116)	0.8025 (±0.0180)	0.6467 (±0.0196)	<b>0.4562</b> (±0.0063)	0.7726 (±0.0269)	0.8003 (±0.0075)	
		NYC	0.5008 (±0.0008)	0.4784 (±0.0016)	0.5341 (±0.0298)	0.7046 (±0.0402)	0.6012 (±0.0169)	0.5100 (±0.0048)	<b>0.4026</b> (±0.0033)	0.5855 (±0.0069)	0.6970 (±0.0095)	
30 days		Trans.	Seoul	<b>0.3924</b> (±0.0020)	0.5949 (±0.0001)	0.7503 (±0.0708)	0.6425 (±0.0006)	0.6446 (±0.0059)	0.4082 (±0.0034)	0.4082 (±0.0095)	0.4215 (±0.0075)	0.6431 (±0.0016)
			Busan	0.5985 (±0.0023)	0.6038 (±0.0004)	0.9622 (±0.0453)	0.9365 (±0.0024)	0.7654 (±0.0241)	0.6424 (±0.0028)	<b>0.5969</b> (±0.0126)	0.6759 (±0.0015)	0.9402 (±0.0001)
			Daegu	<b>0.4750</b> (±0.0004)	0.5006 (±0.0004)	0.8132 (±0.0057)	0.7285 (±0.0021)	0.5849 (±0.0124)	0.4957 (±0.0017)	0.4846 (±0.0023)	0.4923 (±0.0017)	0.7315 (±0.0012)
			NYC	0.4747 (±0.0019)	0.4592 (±0.0004)	0.9075 (±0.0185)	0.723 (±0.0013)	0.5709 (±0.0122)	0.4811 (±0.0022)	<b>0.4054</b> (±0.0040)	0.4627 (±0.0045)	0.6598 (±0.0005)
	Epic.	Korea	0.7035 (±0.0028)	0.6479 (±0.0012)	0.7318 (±0.0504)	1.0122 (±0.0077)	1.1443 (±0.0469)	0.7268 (±0.0197)	<b>0.5049</b> (±0.0118)	0.8537 (±0.0500)	0.8247 (±0.0172)	
		NYC	0.5304 (±0.0014)	0.4875 (±0.0010)	0.5272 (±0.0286)	0.7243 (±0.0138)	0.6370 (±0.0121)	0.5408 (±0.0068)	<b>0.4068</b> (±0.0044)	0.6154 (±0.0189)	0.6932 (±0.0104)	

that GNN-based approaches have the potential to manage complex network relationships and scenarios involving spatio-temporal interactions with more dataset-specific adaptations.

#### 5.4 SUMMARY OF FINDINGS

Overall, the results indicate that no single forecasting model outperforms all others across all datasets. Instead, the choice of the best model depends on the specific characteristics of the dataset and the underlying data patterns. Linear-based models are effective in simpler scenarios, Transformer-based approaches excel in contexts with long-range dependencies, CNN-based methods work well with spatio-temporal data, and GNN-based models are ideal for datasets with complex networks.

- While linear models such as DLinear and NLinear perform well in simpler scenarios, they struggle with more complex data patterns and non-linear relationships. These models are limited in their ability to capture intricate temporal dependencies and are not suitable for datasets with highly dynamic or irregular patterns. However, in our datasets, they are simple but powerful baselines.
- RNN-based models, such as SegRNN, face challenges in handling long-range dependencies and complex temporal patterns. As the sequence length increases, RNNs suffer from vanishing or exploding gradients (Pascanu et al., 2013), limiting their effectiveness in capturing long-term dependencies. Therefore, SegRNN performs badly on our transportation datasets.
- While Transformer-based models like PatchTST demonstrate promising results in handling long-range dependencies, they struggle with capturing local patterns and short-term dynamics. The self-attention mechanism in Transformers can be computationally intensive, especially for longer sequences (Wang et al., 2020), which can limit their scalability. Moreover, Transformers often require large amounts of training data to achieve optimal performance.
- GNN-based models are designed to handle complex network relationships but require careful design and fine-tuning to achieve optimal performance. The performance of GNN-based models

486 heavily depends on the quality and representation of the graph structure, which can be challenging  
 487 to construct for some datasets. Moreover, GNNs can be computationally expensive, especially for  
 488 large-scale networks (Ding et al., 2022) and face scalability issues.  
 489

490 These findings provide a valuable reference for researchers and practitioners when selecting appropri-  
 491 ate forecasting models for their specific applications. The comprehensive evaluation across diverse  
 492 datasets and model architectures reinforces the importance of experimentation and context-driven  
 493 decision-making in the field of mobility networked time-series forecasting. However, the limitations  
 494 of existing forecasting models highlight the need for innovative approaches that can effectively  
 495 address the challenges posed by complex and diverse datasets. That is, a novel approach is anticipated  
 496 to outperform DLinear and TimesNet for this challenging problem.  
 497

## 498 6 FUTURE WORK AND LIMITATIONS

499 The complexity of mobility patterns requires diverse and comprehensive analysis for mobility  
 500 networked time-series forecasting. Therefore, every component of mobility datasets captures spatio-  
 501 temporal variability across multiple transportation modes and organizes the datasets into a bi-modal  
 502 form, facilitating a comprehensive understanding of mobility trends over time. Additionally, the  
 503 structure of the datasets with explainable units under a spatial network increases explainability, aiding  
 504 decision-makers in interpreting mobility trends and implications for urban planning (Li et al., 2012;  
 505 Hoang et al., 2016) and epidemic control (Ni & Weng, 2009; Katragadda et al., 2022) and these  
 506 insights can significantly impact policy-making and economic decisions.  
 507

508 While **MOBINS** dataset collection serves as a forecasting benchmark, the presence of distribution  
 509 shifts due to the changes in the *Epidemic-[Korea, NYC]* datasets suggests that they can be utilized  
 510 for time-series online learning, adapting models in real-time. Additionally, the benchmark can be  
 511 extended for research on imputation, clustering of traveling behaviors, and hierarchical time-series  
 512 forecasting. Despite the advantages of our datasets, there are a few constraints, such as the fact that  
 513 **MOBINS** is limited to only two domains and its period of dataset collection is mostly only two to  
 514 three years, which is not enough to support annual patterns.  
 515

## 516 REFERENCES

- 517 Mucong Ding, Tahseen Rabbani, Bang An, Evan Wang, and Furong Huang. Sketch-GNN: Scalable  
 518 graph neural networks with sublinear training complexity. *Advances in Neural Information  
 519 Processing Systems*, 35:2930–2943, 2022.  
 520  
 521 Fivethirtyeight. Uber TLC FOIL response. [https://github.com/fivethirtyeight/  
 522 uber-tlc-foil-response](https://github.com/fivethirtyeight/uber-tlc-foil-response), 2015. Online; accessed 3-May-2024.  
 523  
 524 Liangzhe Han, Xiaojian Ma, Leilei Sun, Bowen Du, Yanjie Fu, Weifeng Lv, and Hui Xiong.  
 525 Continuous-time and multi-level graph representation learning for origin-destination demand  
 526 prediction. In *Proceedings of the ACM SIGKDD Conference on Knowledge Discovery & Data  
 527 Mining*, pp. 516–524, 2022.  
 528  
 529 Minh X Hoang, Yu Zheng, and Ambuj K Singh. Fccf: Forecasting citywide crowd flows based on  
 530 big data. In *Proceedings of the 24th ACM SIGSPATIAL International Conference on Advances in  
 Geographic Information Systems*, pp. 1–10, 2016.  
 531  
 532 Renhe Jiang, Du Yin, Zhaonan Wang, Yizhuo Wang, Jiewen Deng, Hangchen Liu, Zekun Cai,  
 533 Jinliang Deng, Xuan Song, and Ryosuke Shibasaki. D1-traffic: Survey and benchmark of deep  
 534 learning models for urban traffic prediction. In *Proceedings of the ACM International Conference  
 on Information & Knowledge Management*, pp. 4515–4525, 2021.  
 535  
 536 Satya Katragadda, Ravi Teja Bhupatiraju, Vijay Raghavan, Ziad Ashkar, and Raju Gottumukkala.  
 537 Examining the COVID-19 case growth rate due to visitor vs. local mobility in the United States  
 538 using machine learning. *Scientific Reports*, 12(1):12337, 2022.  
 539  
 539 Nikita Kitaev, Łukasz Kaiser, and Anselm Levskaya. Reformer: The efficient transformer. *arXiv  
 preprint arXiv:2001.04451*, 2020.

- 540 Xiaolong Li, Gang Pan, Zhaohui Wu, Guande Qi, Shijian Li, Daqing Zhang, Wangsheng Zhang,  
541 and Zonghui Wang. Prediction of urban human mobility using large-scale taxi traces and its  
542 applications. *Frontiers of Computer Science*, 6:111–121, 2012.
- 543 Yaguang Li, Rose Yu, Cyrus Shahabi, and Yan Liu. Diffusion convolutional recurrent neural network:  
544 Data-driven traffic forecasting. *arXiv preprint arXiv:1707.01926*, 2017.
- 545 Shengsheng Lin, Weiwei Lin, Wentai Wu, Feiyu Zhao, Ruichao Mo, and Haotong Zhang. Seg-  
546 rnn: Segment recurrent neural network for long-term time series forecasting. *arXiv preprint*  
547 *arXiv:2308.11200*, 2023.
- 548 Xu Liu, Yutong Xia, Yuxuan Liang, Junfeng Hu, Yiwei Wang, Lei Bai, Chao Huang, Zhenguang  
549 Liu, Bryan Hooi, and Roger Zimmermann. Largest: A benchmark dataset for large-scale traffic  
550 forecasting. *Advances in Neural Information Processing Systems*, 36, 2024.
- 551 Shunjiang Ni and Wenguo Weng. Impact of travel patterns on epidemic dynamics in heterogeneous  
552 spatial metapopulation networks. *Physical Review E—Statistical, Nonlinear, and Soft Matter*  
553 *Physics*, 79(1):016111, 2009.
- 554 Yuqi Nie, Nam H Nguyen, Phanwadee Sinthong, and Jayant Kalagnanam. A time series is worth 64  
555 words: Long-term forecasting with transformers. *arXiv preprint arXiv:2211.14730*, 2022.
- 556 Junjie Ou, Jiahui Sun, Yichen Zhu, Haiming Jin, Yijuan Liu, Fan Zhang, Jianqiang Huang, and  
557 Xinbing Wang. Stp-trellisnets: Spatial-temporal parallel trellisnets for metro station passenger flow  
558 prediction. In *Proceedings of the ACM International Conference on Information & Knowledge*  
559 *Management*, pp. 1185–1194, 2020.
- 560 George Panagopoulos, Giannis Nikolentzos, and Michalis Vazirgiannis. Transfer graph neural net-  
561 works for pandemic forecasting. In *Proceedings of the AAAI Conference on Artificial Intelligence*,  
562 pp. 4838–4845, 2021.
- 563 Razvan Pascanu, Tomas Mikolov, and Yoshua Bengio. On the difficulty of training recurrent neural  
564 networks. In *Proceedings of the International Conference on Machine Learning*, pp. 1310–1318,  
565 2013.
- 566 Can Rong, Jingtao Ding, and Yong Li. An interdisciplinary survey on origin-destination flows  
567 modeling: Theory and techniques. *arXiv preprint arXiv:2306.10048*, 2023.
- 568 Hongzhi Shi, Quanming Yao, Qi Guo, Yaguang Li, Lingyu Zhang, Jieping Ye, Yong Li, and Yan  
569 Liu. Predicting origin-destination flow via multi-perspective graph convolutional network. In  
570 *Proceedings of the IEEE International Conference on Data Engineering*, pp. 1818–1821, 2020.
- 571 Utkarsh Singh, Jean-François Determe, François Horlin, and Philippe De Doncker. Crowd forecasting  
572 based on WiFi sensors and LSTM neural networks. *IEEE Transactions on Instrumentation and*  
573 *Measurement*, 69(9):6121–6131, 2020.
- 574 TianChi. Tianchi global urban computing ai competition: Metro passenger flow  
575 prediction. [https://tianchi.aliyun.com/competition/entrance/231708/  
576 introduction/](https://tianchi.aliyun.com/competition/entrance/231708/introduction/), 2019. Online; accessed 1-May-2024.
- 577 TLC. TLC trip record data. [https://www.nyc.gov/site/tlc/about/  
578 tlc-trip-record-data.page](https://www.nyc.gov/site/tlc/about/tlc-trip-record-data.page), 2009. Online; accessed 3-May-2024.
- 579 Dingsu Wang, Yuchen Yan, Ruizhong Qiu, Yada Zhu, Kaiyu Guan, Andrew Margenot, and Hanghang  
580 Tong. Networked time series imputation via position-aware graph enhanced variational autoen-  
581 coders. In *Proceedings of the ACM SIGKDD Conference on Knowledge Discovery & Data Mining*,  
582 pp. 2256–2268, 2023.
- 583 Sinong Wang, Belinda Z. Li, Madian Khabsa, Han Fang, and Hao Ma. Linformer: Self-attention  
584 with linear complexity. *arXiv preprint arXiv:2006.04768*, 2020.
- 585 Yuandong Wang, Hongzhi Yin, Hongxu Chen, Tianyu Wo, Jie Xu, and Kai Zheng. Origin-destination  
586 matrix prediction via graph convolution: a new perspective of passenger demand modeling. In  
587 *Proceedings of the ACM SIGKDD International Conference on Knowledge Discovery & Data*  
588 *Mining*, pp. 1227–1235, 2019.

594 Haixu Wu, Tengge Hu, Yong Liu, Hang Zhou, Jianmin Wang, and Mingsheng Long. Timesnet:  
595 Temporal 2d-variation modeling for general time series analysis. In *Proceedings of the International  
596 Conference on Learning Representations*, 2022.  
597

598 Bing Yu, Haoteng Yin, and Zhanxing Zhu. Spatio-temporal graph convolutional networks: a deep  
599 learning framework for traffic forecasting. In *Proceedings of the International Joint Conference on  
600 Artificial Intelligence*, pp. 3634–3640, 2018.

601 Ailing Zeng, Muxi Chen, Lei Zhang, and Qiang Xu. Are transformers effective for time series  
602 forecasting? In *Proceedings of the AAAI Conference on Artificial Intelligence*, pp. 11121–11128,  
603 2023.  
604

605 Haoyi Zhou, Shanghang Zhang, Jieqi Peng, Shuai Zhang, Jianxin Li, Hui Xiong, and Wancai Zhang.  
606 Informer: Beyond efficient transformer for long sequence time-series forecasting. In *Proceedings  
607 of the AAAI Conference on Artificial Intelligence*, pp. 11106–11115, 2021.  
608  
609  
610  
611  
612  
613  
614  
615  
616  
617  
618  
619  
620  
621  
622  
623  
624  
625  
626  
627  
628  
629  
630  
631  
632  
633  
634  
635  
636  
637  
638  
639  
640  
641  
642  
643  
644  
645  
646  
647